Chapter 8
Nanosized Oxides of Different Compositions as Adsorbents for Hazardous Substances Removal from Aqueous Solutions and Wastewaters

Małgorzata Wiśniewska, Monika Wawrzkiewicz, Anna Wołowicz, and Olena Goncharuk

8.1 Introduction

Due to industrialization and urbanization processes, large quantities of effluents containing hazardous substances are discharged into the environment. Not only inorganic contaminants such as heavy metals, e.g. Cd, Cr, Cu, Ni, As, Pb and Zn, but also organic compounds like phenol (and its salts), polyalcohols, polyacids (and other macromolecular compounds), azo dyes, dioxins, furanes as well as many others are generated by metallurgical, engineering, mining, electroplating, nuclear, chemical, textile, petroleum, plastic, cellulose, etc. industries. Many of them are known to be toxic or carcinogenic. Thus removal of such hazardous substances is of crucial importance to protect the human and the environment. Several techniques have been used to remove organic and inorganic impurities from industrial wastewaters. Recently increasing attention has been focused on adsorption techniques using metal and semimetal oxide sorbents such as aluminium oxide, iron oxide, titanium oxide, manganese oxide, zirconium oxide and silica oxide. The nanosized

M. Wiśniewska (✉)
Department of Radiochemistry and Colloid Chemistry, Faculty of Chemistry, Maria Curie-Sklodowska University, Lublin, Poland
e-mail: wisniewska@hektor.umcs.lublin.pl

M. Wawrzkiewicz · A. Wołowicz
Department of Inorganic Chemistry, Faculty of Chemistry, Maria Curie-Sklodowska University, Lublin, Poland

O. Goncharuk
O. O. Chuiko Institute of Surface Chemistry, National Academy of Sciences of Ukraine, Kyiv, Ukraine

O. Fesenko, L. Yatsenko (eds.), *Nanooptics, Nanophotonics, Nanostructures, and Their Applications*, Springer Proceedings in Physics 210,
https://doi.org/10.1007/978-3-319-91083-3_8

metal, semimetal and mixed oxides are classified as the promising sorbents because of their large surface areas and pore sizes as well as mechanical and thermal stability.

8.2 Properties and Synthesis of Individual and Mixed Nanosized Oxides

Individual and mixed nanosized oxides (NMOs) have become increasingly popular in recent decades due to their unique properties, which ensure the expansion of their application in various fields of chemistry, materials science and industry [1–4]. High specific surface area and high concentration of active surface centres of nanosized oxides provide good adsorption properties with respect to low- and high-molecular-weight adsorbents, such as polymers [5–8], metal ions, dyes, etc. [9–17]. The active surface centres in such nanooxide composites are terminal ≡M-OH groups and bridging groups ≡M-O(H)-M≡ [12, 17–20], which are hydrophilic in nature and possess different Brönsted and Lewis acidities, which ensure the catalytic activity of such nanocomposites in different catalytic processes [21–26] and determine the properties of their surface when interacting with various adsorbents in the atmosphere and aqueous medium. The ability of such groups to dissociate in an aqueous medium provides the formation of a surface charge and a double electric layer [18], which determines such surface properties as ability to adsorb metal ions [16, 17] and dyes, as well as such important properties as electrokinetic potential and colloidal stability of dispersions. In the adsorption interaction with polymers, such a surface charge can play a positive role in the case of interactions with an oppositely charged polyelectrolyte and a negative role in the case of charged electrolyte of the same sign or a nonionic polymer for which such mechanism is realized as the hydrogen bonding with undissociated surface groups. It should be noted that bridging groups of the type $\equiv M_{(1)}\text{-}O(H)\text{-}M_{(2)}\equiv$, which are formed on the surface of mixed oxide composites, differ significantly in properties from the bridging groups of the $\equiv M_{(1)}\text{-}O(H)\text{-}M_{(1)} \equiv$ type. For example, often their Brönsted acidity is often much higher, which determines noticeable differences in the properties of individual highly dispersed oxides and mixed nanocomposites.

Formation of the surface structure is significantly affected by the method of synthesis of mixed oxides: pyrogenic, sol-gel, chemical vapour deposition (CVD), etc. The pyrogenic method is one of the most common due to the convenience of its industrial application [27, 28]. A pyrogenic method of the synthesis of individual and mixed oxides consists in high-temperature hydrolysis of the corresponding metal or metalloid tetrachlorides in a hydrogen-oxygen flame at 1100–1400 °C. The variations of the initial component ratios, temperature and flow rate make it possible to obtain fumed mixed oxide of binary or triple compositions with high specific surface area and different phase ratios. The most common oxides produced by this process are individual and mixed fumed oxides of silicon, titanium and aluminium [17–20]. Also many other fumed oxides, such as GeO_2, Fe_2O_3, Cr_2O_3, MoO_3, SnO_2, V_2O_5, etc., have been produced by Degussa using the pyrogenic method [29].

Fumed nanooxides have proven to be good adsorbents of metal cations and dyes [10, 11, 16, 17], polymers [5–8], etc. Especially effective are mixed systems due to the presence of bridging groups of ≡Si-O(H)-Ti ≡ or ≡Si-O(H)-Al ≡ on their surface, which are significantly stronger Brönsted and Lewis acid sites than the terminal OH groups and bridging groups of the $\equiv M_{(1)}$-O(H)-$M_{(1)} \equiv$ type and vastly affect the properties of the nanocomposite surface [17–20]. Mixed fumed oxides are unevenly distributed in the bulk and on the surface. Thus for the Al_2O_3/SiO_2 and ternary $Al_2O_3/TiO_2/SiO_2$ systems, the phase of Al_2O_3 is maximally concentrated in the surface layer of the nanocomposite with a low Al_2O_3 content (3–10% wt.). The surface concentration of TiO_2 increases monotonously with the increasing TiO_2 content in the TiO_2/SiO_2 and ternary nanocomposites. There is mutual influence of the components on formation of the structure in synthesis process. Thus Al_2O_3 has a completely amorphous state in the Al_2O_3/SiO_2 nanocomposite in contrast to the individual fumed Al_2O_3, which includes 20% of the γ-phase. The presence of anatase and rutile in the phase structure is observed in TiO_2 and TiO_2/SiO_2, but their ratio can vary depending on the TiO_2 content in the composite. The high temperature during the pyrogenic synthesis prevents the formation and growth of large crystallites, thereby achieving a nanoscale structure. In the case of tendency to form a crystalline structure in binary oxides, for example, as in the case of TiO_2/SiO_2, each oxide forms its own phase with formation of bridge bonds of the $\equiv M_{(1)}$-O(H)-$M_{(2)} \equiv$ type at the phase boundary.

At the same time, in the formation of an amorphous structure, as in the case of alumina-silica, a more uniform distribution of oxides occurs in the surface layer of the composite with formation of a significant number of bridge bonds of the$\equiv M_{(1)}$-O(H)-$M_{(2)} \equiv$ type.

To accomplish obtaining the core-shell nanoscale structure, the CVD method [23–32] is applied, i.e. a layer of the second oxide is deposited from the vapour phase on the already synthesized nanoparticles of the carrier oxide. This method has many features associated with the structure formation of the second oxide on the core-oxide surface. Thus in most cases, it is not possible to form a continuous layer of the second oxide since it forms a crystalline or amorphous cluster structure [32]. Thus the surface structure of the CVD-synthesized oxide composite includes both the support and supported oxide surface areas, the ratio of which determines the surface properties of the mixed oxide.

The deposition of the second oxide onto the carrier oxide can also be carried out from the liquid phase using water, hexane, etc. as the solvents. Silica-supported nanocomposites with CeO, ZrO, TiO_2 and Fe_2O_3 were synthesized by this method [21, 33–37]. It was reported also in [22] as regards some other oxides, such as Mg, Mn, Ni, Cu and Zn oxides, deposited on fumed silica. Depending on the deposited oxide concentration, it is possible to obtain a layer of another oxide on the carrier oxide surface, or the carrier becomes a matrix for the growth of particles of a separate second phase at a higher content of the deposited oxide. In this case only a small fraction of the surface of the carrier oxide interacts with the synthesized oxide. This method is generally used to control the growth of the second phase particles due to the presence of a carrier oxide.

Another common method of synthesis using solvent is the sol-gel synthesis. The sol-gel process is a well-established colloidal chemistry technology; the process occurs in the liquid solution of organometallic precursors (TMOS, TEOS, Zr (IV) propoxide, Ti(IV) butoxide, etc.) and results in formation of a new phase of nanooxides by means of hydrolysis and condensation reactions. The main advantages of the sol-gel method are high purity and homogeneous nanostructure with predefined material properties at relatively low process costs. A lot of papers reported on the study of sol-gel synthesis conditions and properties of the obtained silica nanoparticles [38], zinc oxide [39], titanium dioxide [40] and mixed oxide nanocomposites [41].

Thus the variety of synthesis methods provides the possibility of obtaining highly dispersed oxide materials with diverse morphology and surface properties that are promising sorbents for such types of pollutants as ions of heavy metals, dyes, etc.

8.3 Single, Mixed and Modified Nanosized Oxides as Adsorbents

8.3.1 Metal Ions

Among the toxic pollutants introduced into the environment by humans as a result of progressing urbanization and industrialization processes, heavy metals are particularly dangerous. In the second half of the twentieth century, increased interest in heavy metals and their impact on human organisms as well as on aquatic ecosystems were observed. The main sources of heavy metals in the environment are natural and anthropogenic ones. Circulation and migration of heavy metals in the natural environment are mainly related to such processes as weathering rocks, eruption of volcanoes, evaporation of oceans, forest fires and soil-forming processes. On the other hand, anthropogenic sources of heavy metals included activity of various branches of industries, transport, municipal economy, waste landfill, chemical industry, fertilizers and wastes used for fertilization, energetics based on coal and lignite combustion, ore mining, metallurgy and exhaust fumes [42, 43]. The problem of heavy metal pollution largely concerns industrialized areas which produce a large amount of wastewaters coming from mining, hydrometallurgy, textiles, paint and pigment production, mineral fertilizers and plant protection products, rubber and plastics, wood products, etc. [44–46] (Fig. 8.1).

The heavy metals that come from these sources are dispersed into the environment in an uncontrolled way resulting in atmosphere, surface, groundwater and soil pollution [47]. Their ability to circulate in the environment and enter the food chain results in a particular risk to plant, animal and human organisms. Heavy metals are involved in the biogeochemical circulation which is part of the biological circuit (flow of elements in the trophic chain) where the first link being a plant, the next animal and the last one human (soil → plant → animal → human). Moving the

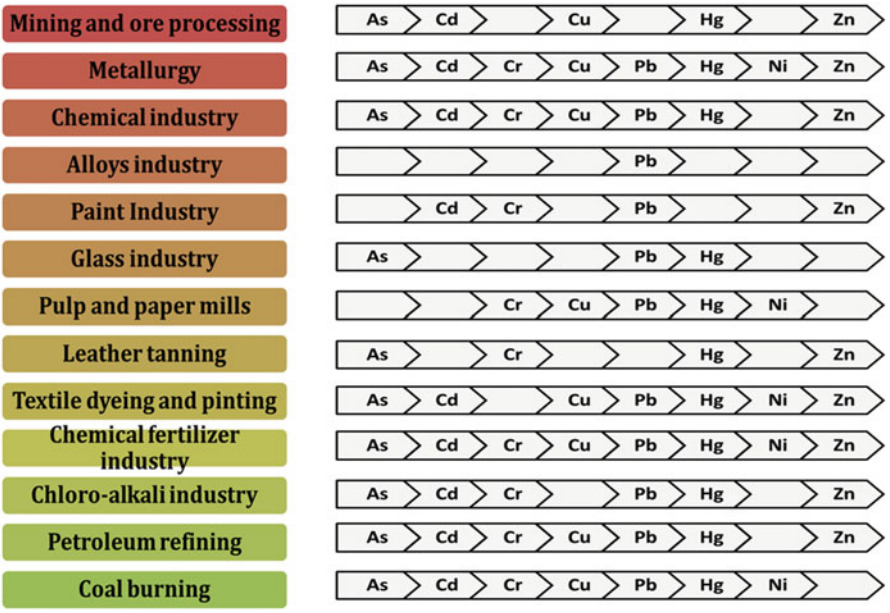

Fig. 8.1 Sources of heavy metals

metals to the next link results in an increase in concentration, resulting in a partial accumulation of these elements in a given cell. Heavy metals accumulate in the last link, the human body. Moreover, their high durability and long half-life, e.g. duration in soil >1000 years, non-biodegradability, biomagnification, chronicity, synergic effect, teratogenicity and mutagenicity result in serious health problems [42, 44, 48]. Long-term effects of heavy metals on the human body or acute toxicity can cause damage to the central nervous system, problems with the cardiovascular and gastrointestinal systems and damage to the internal organs, e.g. the liver, kidneys and lungs, and can enhance the risk of some cancers, etc. [43, 44, 49]. Taking into account danger of heavy metals, they can be divided into (a) very high, Cd, Hg, Pb, Cu, Zn and Cr; (b) high, Mo, Mn and Fe; (c) medium, Ni and Co; and (d) low degrees of potential risk, Sr and Zr. Hazards of bioaccumulation of heavy metals in the environment determine the need for their removal. Despite the existence of various methods of wastewater treatment, among others, membrane filtration, electrodialysis, photocatalysis, chemical precipitation, coagulation, flocculation, reverse osmosis or oxidation and new and effective ways of removing heavy metal ions from wastewaters are still searched for [44, 45, 50–52]. Among these techniques, sorption has come to the forefront as one of the major techniques for heavy metal removal from wastewaters due to flexibility in design and operation, possibility of generating high-quality treated effluents, high efficiency, metal selectivity, ease of operation, high regeneration and reuse of sorbent, low-cost maintenance, etc. [52, 53]. Heavy metal removal from water and wastewaters can be accomplished by sorption

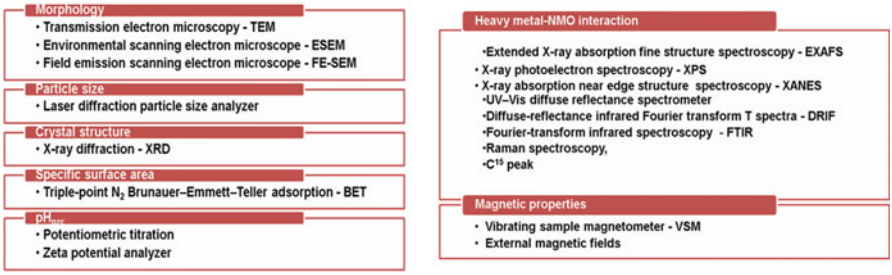

Fig. 8.2 Methods applied for NMO characterization

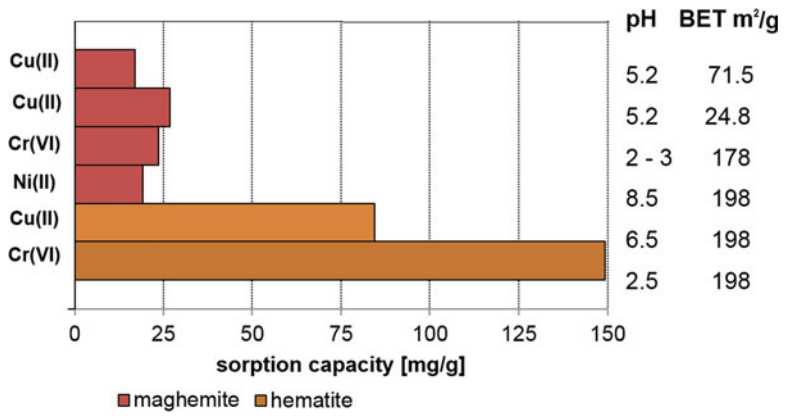

Fig. 8.3 Comparison of NFeO capacities for heavy metal ions [50, 57, 58]

processes using promising nanosized metal oxides such as aluminium, silica, ferric, manganese, titanium, magnesium, cerium oxides, etc. of which the most widely studied are iron oxides, manganese oxides, aluminium oxides and titanium oxides [50]. In order to understand the mechanism of the sorption process on oxides (interactions in the NMO-heavy metal system) and to compare the removal efficiency of these pollutants, it is extremely important to gather detailed information about the surface morphology of oxides, particle size, BET surface area, magnetic properties and crystalline structure. Such information about NMOs can be obtained using various techniques and methods presented in Fig. 8.2 [50, 54, 55].

Due to the wide use of NMOs as effective sorbents of heavy metal ions in the literature, a number of papers devoted to this subject and review ones can be found [50, 54–56]. For this reason only selected NMO applications are presented and cited below. Widespread of iron, reuse of resources, being eco-friendly and ease in the synthesis make nanosized ferric oxide (NFeOs) a common sorbent for heavy metal removal. In this group of NFeOs, goethite (α-FeOOH), hematite (α-Fe_2O_3), magnetite (Fe_2O_4), maghemite (γ-Fe_2O_3), amorphous hydrous FeOs and iron/iron oxide are frequently used [50, 57, 58] (Fig. 8.3). As it was observed, divalent metal cations

usually form inner-sphere surface complexes with NMOs. In the case of hydrous ferric oxide (HFOs), the sorption processes seem to be poorly sensitive to ionic strength variation, e.g. Cu(II) and Pb(II) sorption on HFOs (0.0005–0.5 M $NaClO_4$) [59] and Pb(II) sorption on ferrihydrite (0.001–0.1 M $NaNO_3$) [60], which might suggest also inner-sphere complex formation. Sorption of Cr(VI), Cu(II) and Ni(II) on maghemite is strongly pH-dependent [57], and under optimal pH electrostatic attraction, a mechanism similar to Cr(VI) sorption onto maghemite was observed [50].

Nanosized manganese oxides (NMnOs), e.g. hydrous manganese oxide (HMO) [61–65], mixed-valence manganese oxide, nanotunnel manganese oxide (octahedral molecular sieve, OMS-1 or OMS-2) [66, 67], were applied for Cs(I) [61], Hg(II) [62], As [63], Cd [64], Pb(II), Cd(II), Zn(II) [65], radionuclides [66] and hydrometallurgical wastewater (Al, Ca, Fe, Mg, Mn, Na) [67] removal. As was pointed out, hydrous manganese oxide similar to HFO forms inner-sphere complexes with metal (M(II)), and ion exchange process takes place during the sorption processes. Moreover, the sorption process includes two steps such as rapid metal adsorption on the external surface and slow intraparticle diffusion along the micropore walls [65]. Additionally, HMO active sites are heterogeneous due to the fact that the sorption is better represented by the Freundlich isotherm model [65]. In the case of tunnelled manganese oxide, their sorption ability is strongly dependent on their structure [66].

The other popular oxides for heavy metal ion removal are aluminium, titanium and zinc ones [68]. As it was found, aluminium oxide can be chemically or physically modified which allows to introduce additional functional groups containing donor atoms, e.g. O, N, S and P, which improve removal efficiency of heavy metal ions. Modification of γ-Al_2O_3 by γ-mercaptopropyl-trimethoxysilane (γ-MPTMS) in the presence of sodium dodecyl sulphate (SDS) improves removal efficiency of Zn(II), Pb(II), Cu(II) and Fe(III) from 55, 36, 27 and 24% (Al_2O_3 1 g, SDS 50 mg, without MPBIM) to 100, 98, 97 and 96% (Al_2O_3 1 g, MPBIM 40 mg, SDS 50 mg). Surfactant-coated alumina modified by dithizone for Pb(II) sorption [69] or surfactant-coated alumina with immobilized 1,10-phenantroline for Cu(II) and Cd(II) determination [70], γ-Al_2O_3 modified by dinitrophenylhydrazine (DNPH) for Pb(II), Co(II), Cr(III), Cd(II), Ni(II) and Mn(II) sorption [71] was also applied. During the sorption process, metal sorbs on the surface through surface interactions or/and chemical-bonding interactions take place. In the case of alumina modified by γ-MPTMS, three mechanisms of sorption can be found: (a) interactions between thiol groups and metal ions, (b) hydrolyzation of metal ions and (c) electrostatic sorption. Depending on pH of the solution, mechanism (a) plays a more significant role in the case of acidic solutions, whereas for basic solutions mechanisms (b) and (c) are dominant.

As it was mentioned above, titanium and zinc oxides are also found in application in heavy metal removal due to their unique advantages, e.g. simple and cheap to prepare and convenient to tailor morphologically. Some examples of the results of heavy metal sorption on titanium and zinc oxide can be found in Table 8.1.

Table 8.1 Titanium and zinc oxide application in heavy metal removal

Metal oxide	Characteristics	Heavy metals	Performance	Additional information	References
TiO_2 Commercially available	33% titanium and 67% oxygen BET surface area 185.5 m^2/g Particle sizes 8.3 nm	Pb(II), Cd(II), Ni(II)	Pb(II) removal efficiency 100% Cd(II) removal efficiency 99.9% Ni(II) removal efficiency 99.2% 0.5 g/L TiO_2, nano- TiO_2	Langmuir isotherm/modified first order	[72]
TiO_2	Pore diameter 10–50 nm, BET surface area 208 m^2/g	Zn(II), Cd(II)	Zn(II) 15.3 mg/g Cd(II) 7.9 mg/g, pH = 9.0	–	[73]
TiO_2	Pore diameter 12 nm, BET surface area 45.4 m^2/g	Cd(II),Cu(II), Ni(II), Pb(II)	pH_{PZC} values 7.4 120.1, 50.2, 39.3, 21.7 mg/g for Cd(II), Cu(II), Ni(II), Pb(II)	Freundlich model in single- and multiple- component solutions	[74]
ZnO	Pore diameter 5–20 nm, BET surface area 147 m^2/g	Cu(II)	> 1600 mg/g	Freundlich model	[75]
ZnO/PbS	Heterostructured functional nanocomposite, nanosheets	Pb(II)	Pb(II) 6.7 mg/g	–	[76]
ZnO	50 nm (spheroid)	Cd(II), Cu (II), Ni(II), Pb(II)	360.6 mg/g (sum of four metals) in multiple- component solutions	Selectivity series Cd(II) > Pb(II) > Cu(II) – single solutions, Pb(II) > Cu(II) > Cd(II) > Ni(II) – multiple-component solutions	[77]

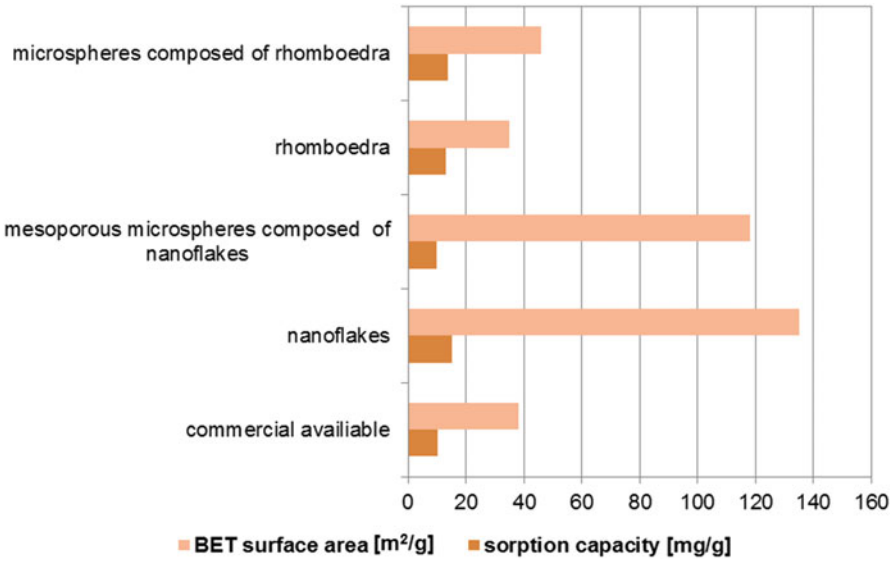

Fig. 8.4 Comparison of sorption capacities obtained for Cr(VI) on NMgOs of various morphologies

Nanosized magnesium oxides (NMgOs), e.g. nanorods, nanowires, nanotubes, nanobelts, nanocubes, etc., of various morphologies were obtained. Then their sorption behaviours towards heavy metal ions were examined, e.g. chromium removal by MCH (magnesium carbonate hydrate) of the phase structure from monocyclic ($Mg_5(CO_3)_4(OH)_2(H_2O)_4$) to hexagonal ($MgCO_3$) [78]. As it was found, both nanoflakes and flowerlike microspheres ensure very good adsorption efficiency (Fig. 8.4). After 120 min of phase contact time, the concentration of Cd(II) and Pb(II) decreased significantly from 100 mg/L to 0.007 mg/L and 0.05 mg/L, respectively.

Nanosized cerium oxide sorption behaviour depends on the size, shape, morphology and surface area [50, 79]. Cr(VI) sorption on the CeO_2 nanoparticles (synthesized by oxidation of Ce(III) nitrate under basic conditions using hexamethylenetetramine) of the mean size 12 nm and the BET surface area shows that after the sorption process, Cr(VI) was not present in the solid phase (only Cr(III) was present), whereas in the liquid phase, Cr(VI) exists. This fact indicates that on the surface of nanoparticles, the Ox-Red process can be possible and reduction of chromium takes place. The sorption process of chromium can be described by the pseudo-second-order kinetic equation and the Freundlich model [80]. Similarly to magnesium oxide, cerium oxide can be also obtained in different morphological forms. Ceria hollow nanospheres obtained by the hydrothermal method of nanocrystal size 14 nm and the BET surface area of 72 m^2/g give nearly 70 times higher sorption capacities for Cr(VI) 15.4 mg/g and Pb(II) 9.2 mg/g than the commercial bulk ceria material. The isotherm was well described by the Langmuir isotherm

model. Removal of Cd(II), Pb(II) and Cr(VI) ions in single- and three-component solutions using cerium oxide (CeO_2) nanoparticles was carried out by Contreras et al. [81]. The highest percentage of removal was obtained in the case of Pb(II) adsorption capacity which was equal to 128.1 mg/g, then for Cd(II) 93.4 mg/g and finally for chromium(VI) 34.4 mg/g. pH effect (pH = 5, pH =7) on % removal efficiency was observed for Cd(II) and Cr(VI), whereas in the case of Pb(II), the pH effect was not pointed out. Additionally, sorption capacities were not affected by the type of system (single or three component).

Due to the possibility of agglomeration of NMOs, which results in loss of activity and pressure drop when used in the column systems as well as difficulty in separation, attempts are made to overcome these disadvantages by obtaining hybrid adsorbents impregnating or coating NMOs into/onto a larger size porous support forming an NMOs-supported host [50]. As the host support of NMOs for heavy metal removal, there can be applied natural supports, e.g. raw bentonite (RB), sand, montmorillonite and metallic oxide, as well as manufactured polymer supports [50]. Eren applied iron-coated (ICB, iron-coated bentonite) or magnesium-coated (MCB, magnesium-coated bentonite) RB for Pb(II) removal. The sorption capacities for Pb(II) were in the following order: RB 16.7 mg/g < ICB 22.2 mg/g < MCB 31.86 mg/g (Langmuir capacities) [50, 82]). The sorption yield of Pb(II) using bentonite increases with the pH increase (competition between H^+ and Pb(II) of exchange site can proceed), whereas with the ionic strength increase from 0.01 to 0.1 M Pb(II), the adsorption yield significantly decreases [50]. The presence of Cl^- anions also affects the Pb(II) sorption efficiency which results in different Pb (II) complexes. MCB was also applied for Cu(II) sorption. In this case sorption also depends on the kind of adsorbent surface; Cu(II) forms in the solutions as well as on pH of solutions. For Cu(II) on MCB, the sorption capacities can be presented in the following order: RB 42.41 mg/g < MCB 58.44 mg/g [83]. The other examples of supported NMOs for heavy metal removal from water, e.g. anodic alumina membrane, activated carbon, aluminium oxide, polymeric cation exchanger, etc., are reported in [50].

Magnetic sorbents based on NMOs for heavy metal removal can be also found in the literature [50, 84–86]. In the case of magnetic sorbents, modification of magnetic NFeOs can proceed by the amino, zeolite, poly(3,4-ethylenedioxythiophene) (PEDOT) groups, carbon nanotubes, humic acid, acrylic acid, alginic acid, hydrogel, SiO_2, graphene nanosheets, etc. Such modification prevents from air oxidation and particle aggregation.

8.3.2 Dyes

Intense development of many industries using dyes and pigments to colour their products directly contributes to pollution of the aquatic environment with these substances. Figure 8.5 shows the dyes consumption in various branches of industry in recent years [87–93].

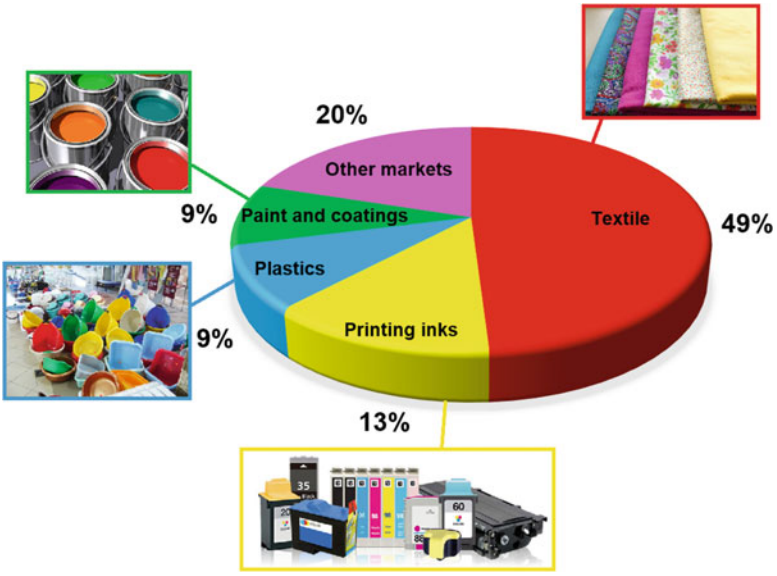

Fig. 8.5 Dyes consumption in different industries

Adsorption methods have a well-established position in the dyes wastewater treatment technology. Adsorbents composed of inorganic oxides such as SiO_2, TiO_2, Al_2O_3, Fe_2O_3, MgO or CaO are frequently used in removal processes of dyes from aqueous solutions. By altering the composition of oxide adsorbents, it is possible to remove different types of dyes, i.e. acid, reactive, direct or basic. An important feature of NMOs is the ability to modify their surface with different reagents, which allows to introduce new functional groups and obtain totally different materials of high quality and functionality. Taking into account the valuable morphological and microstructural properties of NOMs as well as mechanical strength and non-toxicity in many cases, these sorbents become increasingly popular every year in textile effluent treatment [94]. In addition, they are increasingly used as substrates for the synthesis of modern hybrid materials applied for wastewater treatment.

Decolourization of model solutions and raw wastewaters containing dyes from different industrial branches has been studied by many research teams all over the world. The selected results of studies on the use of mixed oxides for dyes removal are presented below.

The mixed nanooxides of Ti and Si (241 m^2/g) and Ti, Al and Si (433 m^2/g) are characterized by high adsorption capacities for basic dyes such as methylene blue and rhodamine 6G [95]. According to Pal et al. [95], the maximum adsorption capacity of the mixed oxide containing Ti and Si for methylene blue was found to be 162.96 mg/g. It is worth noting that the maximum adsorption capacity of the mixed Ti and Si oxide is almost 2.5 times higher than the adsorption capacity of the

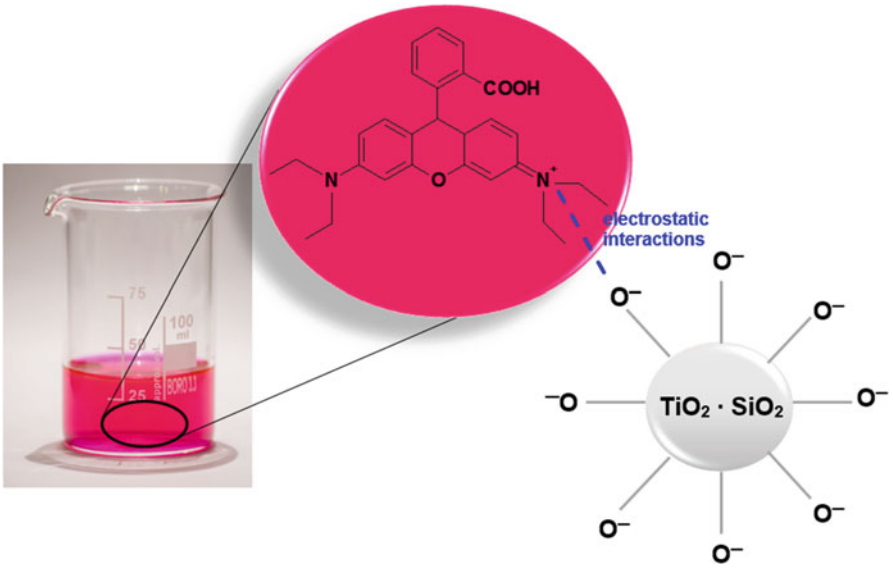

Fig. 8.6 Mechanism of interactions of rhodamine B with the surface hydroxyl groups of mixed TiO_2-SiO_2 oxides of different compositions under the experimental conditions at pH 5–7

mixed oxide containing Ti, Al and Si (65.78 mg/g). The slightly lower value of the adsorption capacity of the mixed Ti and Si oxide equal to 142.9 mg/g was found.

Rasalingam et al. [96] synthesized mesoporous titania-silica oxides of different compositions for rhodamine B adsorption. Among the prepared titania-silica oxides, the highest adsorption capacities were observed for the X-TiSi-03 (TiO_2:SiO_2 = 1:2) and X-TiSi-04 (TiO_2:SiO_2 = 1:3) sorbents which are related to large pore volumes of 0.56 and 0.58 cm^3/g, respectively. The monolayer sorption capacities calculated from the Langmuir adsorption model were found to be 41.2 mg/g for X-TiSi-03 and 44.1 mg/g for X-TiSi-04. The sorption of rhodamine B (Fig. 8.2) under pH 5–7 on these materials occurs as a result of the electrostatic interactions between the surface hydroxyl groups (–OH) of TiO_2·SiO_2 and the positively charged diethylamino groups of the dye as shown below (Fig. 8.6). The presence of oxygen bridges Ti-O-Si also favours adsorption of rhodamine B.

A more complex mechanism of interactions between the dye molecules and silica-based nanocomposite was postulated by Tanzifi et al. [97]. Adsorption of the diazo dye Amido Black B and polyaniline/SiO_2 is a result of interactions between hydroxyl, imine and amine functionalities of the oxide-based sorbent and the amine, hydroxyl and azo groups of Amido Black B. Not only the electrostatic but also van der Waals and hydrogen bonding can exist between these groups. Chemisorption of Amido Black B on the polyaniline/SiO_2 was confirmed by the kinetic studies. The applicability of the pseudo-second-order equation for description of the data was verified by the value of the determination coefficient (r^2 = 1). The surface area, total pore volume and pore diameter for the polyaniline/SiO_2 were determined as 13.36 m

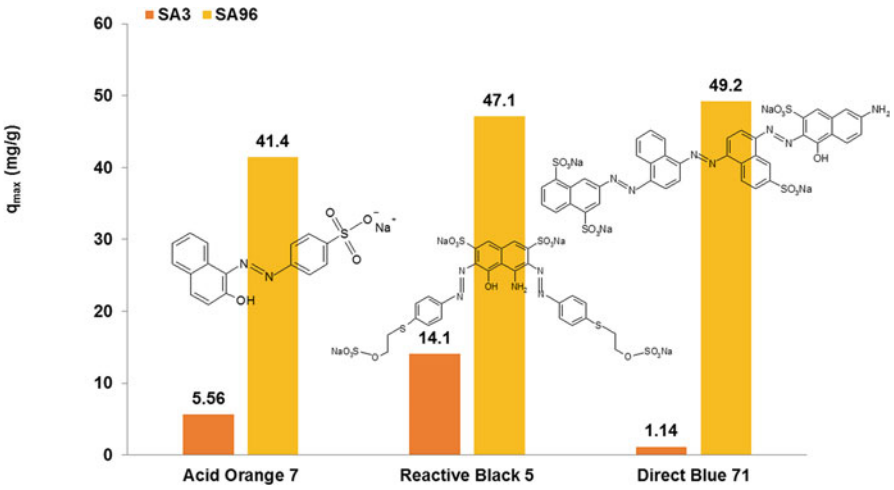

Fig. 8.7 Comparison of maximum sorption capacities of SA3 and SA96 oxides for three textile dyes

^{2}/g, 3.07 cm^3/g and 15.37 nm, respectively. Not only these parameters but also medium pH, adsorption time, temperature and mass of the sorbent influenced Amido Black B adsorption. The adsorption efficiency decreased from 98.6% to 96.8% with the increasing solution pH from 2 to 10. The equilibrium time of adsorption was equal to 60 min. Thermodynamic studies revealed that the retention of Amido Black B on the polyaniline/SiO_2 was endothermic.

SiO_2-Al_2O_3 mixed oxide modified by ferrocene was applied for methyl orange removal by Arshadi et al. [98]. The modified SiO_2-Al_2O_3 (Si/Al-Fe) was a more efficient adsorbent for methyl orange removal (89.0%) after 30 min compared with the non-modified SiO_2-Al_2O_3 (only 4.2% of dye was removed). The maximum adsorption capacity of Si/Al-Fe was equal to 381.0 mg/g. The process followed the pseudo-second-order kinetic model and was spontaneous and endothermic.

Two NMOs composed of SiO_2 and Al_2O_3 were applied for three textile dyes such as Acid Orange 7, Reactive Black 5 and Direct Blue 71 removal from aqueous solutions and wastewaters [10, 11, 99]. The percentage of silicon dioxide in the sorbents was 97% (SA3) and 4% (SA96). The mixed oxides were synthesized using the pyrogenic method which allows to obtain high concentration of Si-O-Al groups on the surface. The maximum sorption capacities (q_{max}) of both oxides for the above-mentioned textile dyes are shown in Fig. 8.7 [10, 11, 99].

It is important to emphasize the highest SA96 sorption capacity for the direct dye (49.2 mg/g). It was noticed that Direct Blue 71 adsorption on SA96 decreased in the presence of the anionic surfactant sodium dodecyl sulphate (SDS), whereas sodium chloride did not influence the retention of the dye [11]. The impact of auxiliaries such as surfactants and electrolytes on dye removal is very important because these substances are frequently present in industrial wastewaters originating from textile plants. The proposed adsorption mechanism of Direct Blue 71 dye on SA96

involved both the electrostatic interactions and hydrogen bonding. In paper [11] it was also confirmed that the mixed oxide SA96 can be applied for decolourization of raw textile wastewaters; 30% reduction of colour was observed after 96 h of contact time.

8.3.3 Polymers

Polymers soluble in the aqueous medium find a wide usage in many branches of industry, environmental protection and agriculture. Acrylic acid polymers (e.g. poly (acrylic acid), PAA, copolymer of acrylic acid with acrylamide-anionic poly(acrylamide), PAM) are used as fillers in washing powders. They function as chelating agents, i.e. remove calcium and magnesium ions. They are applied as dispersants, foaming agents, thickeners, boiler scale inhibitors and flocculants. They are also used as auxiliaries for the paper and textile industries and wastewater treatment and as aids for the extraction of crude oil [100, 101]. The high-molecular-weight polyacrylamides (especially of ionic character) act as effective agents preventing soil erosion and improving textural structure of arable soils. Additionally, poly(vinyl alcohol), PVA polymers and copolymers have important biomedical and pharmaceutical applications [102]. The PVA hydrogels have been studied as candidates for the tissue replacement material for soft contact lenses, artificial heart linings, artificial cartilages, catheters, skin and pancreas membranes. They are also components of drug delivery systems in oral, transdermal, buccal, intramuscular and rectal routes of administration. Moreover, PAA and PVA are excellent polymeric carriers for proteins, enzymes, drugs and other biologically active substances.

Such extensive use of polymers is associated with their presence in municipal and industrial effluents. The basic method of their removal is adsorption on different kinds of adsorbents, including mixed oxides.

The adsorption properties of four mixed oxides of the Me_xO_y-SiO_2 type (Me, metal atom: Mg, Cu, Mn or Zn) in relation to poly(vinyl alcohol) with the average molecular weight 100,000 and the content of acetate groups equal to 14% were examined [5, 6, 103]. NMOs including silica and a given metal oxide were characterized by different contents of metal oxide, i.e. 0.2 and 1 mmol/g SiO_2. Thus they were designated as 0.2 Me_xO_y-SiO_2 and 1 Me_xO_y-SiO_2, respectively.

As can be seen in Fig. 8.8 at pH 6, PVA shows similar affinity for the surfaces of all examined mixed oxides of which the highest adsorption of the polymer was obtained for 1 Mn_xO_y-SiO_2 (approx. 0.4 mg/m^2). Additionally, for all studied systems, the adsorbed amount of polyalcohol increases with the increasing content of metal oxide in the mixed oxide structure. The electrokinetic data proved that the solid surface group containing metal atoms (-Si-O-Me) [104] exhibits preferential adsorption properties of the polymer in relation to the silica hydroxyl ones (-Si-O-H). For this reason a greater number of possible connections between the polymer segments and the -Si-O-Me groups can be formed. As a result, the polymer adsorption increases with the increasing metal oxide content in the silica hybrid material.

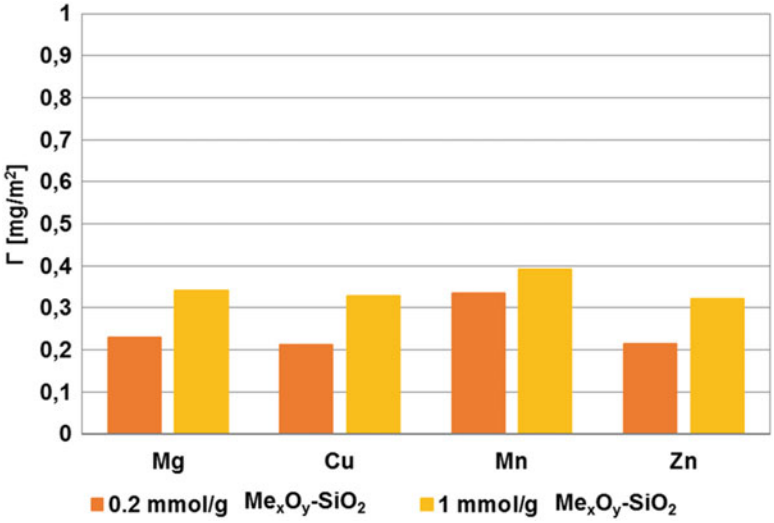

Fig. 8.8 Adsorbed amounts of poly(vinyl alcohol) PVA 100,000 on Me_xO_y-SiO_2 surface (initial polymer concentration 100 ppm, pH 6)

Under natural pH conditions (pH 6), the PVA binding with the mixed oxide surface is mainly of electrostatic nature (points of zero charge (pzc) for all Mn_xO_y-SiO_2 adsorbents are at the pH values higher than 6) [5, 6, 103]. Under such conditions the electrostatic attraction between the negatively charged macromolecules (containing ionized acetate groups) and the positive solid surface (coming from the silica $SiOH_2^+$ groups and metal -Si-O-$MeOH_2^+$ ones) occurs.

The significantly greater adsorption of poly(vinyl alcohol) reaching 0.7 mg/m^2 was obtained on the surface of ternary alumina-silica-titania (Al_2O_3-SiO_2-TiO_2, AST) mixed oxide (Fig. 8.9). Two AST oxides differed in composition – AST50 consisted of 50% TiO_2, 28% SiO_2 and 22% Al_2O_3 whereas AST71 71% TiO_2, 8% SiO_2 and 21% Al_2O_3 were applied (Fig. 8.9).

The amount of adsorbed PVA on the AST surface depends on the solution pH – the decrease of poly(vinyl alcohol) adsorption with the increasing pH for AST50-containing system and the increase of PVA adsorbed amounts with the pH rise on the AST70 surface occur. This is due to specific conformation of the adsorbed macromolecules on the surfaces of examined oxides (with different types of active sites) [105, 106]. The concentration of the hydroxyl surface groups of the mixed oxide, both neutral (-MeOH) and charged (-$MeOH_2^+$, -MeO^-), where Me means Al, Si and Ti atoms, changes with the pH increase. AST50 oxide was characterized by the pH_{pzc} and pH_{iep} (isoelectric point) values equal to 4.8 and 5.8 whereas AST70 by 4.2 and 8.6, respectively. These differences, especially considerable between the diffusion parts of electrical double-layer composition (manifested by pH_{iep} position), change significantly adsorption properties of AST mixed oxides and influence efficiency of PVA removal from aqueous solutions of varying pH values.

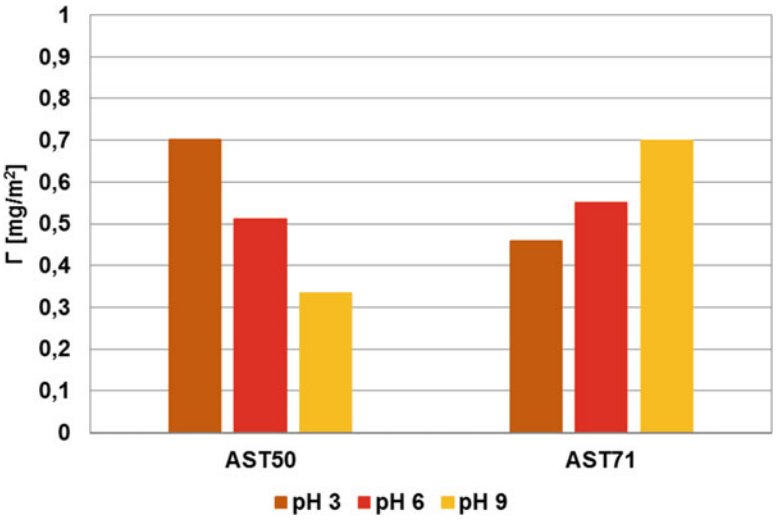

Fig. 8.9 Adsorbed amounts of poly(vinyl alcohol) PVA 100,000 on the Al_2O_3-SiO_2-TiO_2 surface (initial polymer concentration 100 ppm)

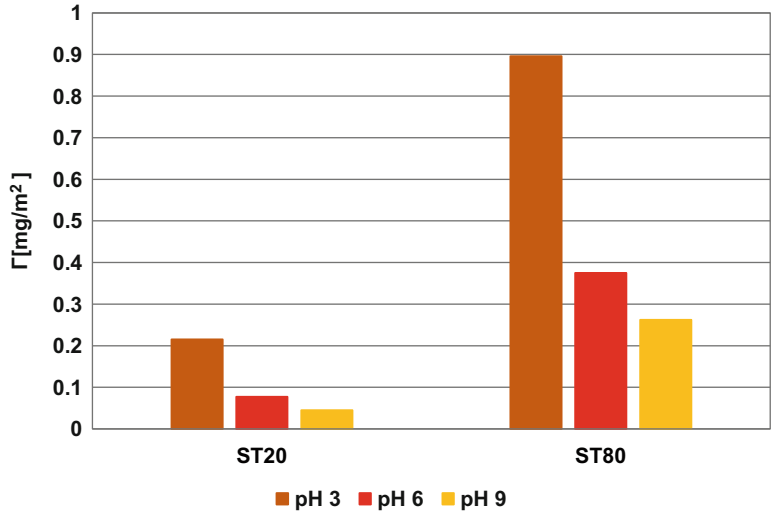

Fig. 8.10 Adsorbed amounts of anionic polyacrylamide PAM 15,500,000 on the SiO_2-TiO_2 surface (initial polymer concentration 100 ppm)

Two mixed silica-titania oxides were also used for the anionic polyacrylamide, PAM adsorption (Fig. 8.10). The polymeric substance was characterized by the average molecular weight 15,500,000 Da and the content of carboxyl groups equal to 50%. The composition of SiO_2-TiO_2, ST oxides was as follows: ST20, 80% SiO_2 and 20% TiO_2 and ST80, 20% SiO_2 and 80% TiO_2.

As can be seen in Fig. 8.9, the adsorption properties of silica-titania mixed oxide in relation to anionic polyacrylamide are determined by the solid composition. This polymer exhibits significantly greater affinity for the surface of the mixed oxide containing 80% of TiO_2. The main reason for this can be a greater tendency of polymeric functional groups (especially carboxyl and amide – to the lesser extent [107]) to interact with the surface groups combined with titania atoms. In such a case, the PAM macromolecules assume flatter conformation on the ST20 oxide surface (characterized by a small content of TiO_2). It limits considerably the accessibility of other polymeric chains to the solid surface and leads to the decrease in PAM adsorbed amounts. Due to the fact that anionic polyacrylamide contains as much as 50% of dissociable carboxyl groups, its interfacial behaviour is influenced by the solution pH. For both examined ST oxides, the greatest adsorption level of PAM is observed at pH 3, at which the favourable electrostatic interactions between the solid and the polymer occur (pH_{pzc} values were 3.8 and 4.8 for ST20 and ST80, respectively). The attractive interactions were observed between the slightly negatively charged macromolecules (small dissociation of PAM carboxyl groups) and the oppositely charged surface hydroxyl groups.

Similar tendencies were observed in the SiO_2-Al_2O_3/poly(acrylic acid) system [108], which is presented in Fig. 8.11. Each segment in the poly(acrylic acid) PAA chain contains the carboxyl functional group (characterized by the pK_a value 4.5). The composition of the SiO_2-Al_2O_3, SA adsorbents was SA3, 97% SiO_2 and 3% Al_2O_3 and SA96, 4% SiO_2 and 96% Al_2O_3. These oxides had the following pH_{pzc} values: 3.4 for SA3 and 7.6 for SA96.

It should be noted that under unfavourable electrostatic forces between the adsorbate and the adsorbent, the polymer adsorption on the mixed oxide surface

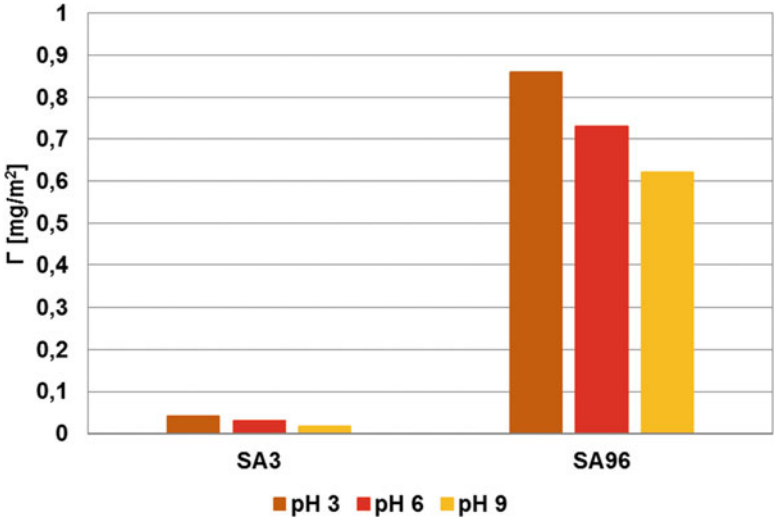

Fig. 8.11 Adsorbed amounts of poly(acrylic acid) PAA 240,000 on the SiO_2-Al_2O_3 surface (initial polymer concentration 100 ppm)

proceeds through the hydrogen bridges and chemical bonds [109]. Carboxyl groups of the polymer can act both as a donor and an acceptor of protons. In such a situation, their binding with the solid surface can take place between all types of adsorbent groups (negative, positive and neutral) and undissociated and dissociated PAA functional groups.

8.4 Conclusions

In the development of inorganic and organic substances such as metal ions, dyes and polymers, the adsorbents possessing not only high adsorption capacity but also by relatively low cost, are largely expected in both science and technology. As was shown above, different NMOs are widely used for their removal from water and wastewaters. Despite various advantages of NMOs, there still exist some technical bottlenecks which should be solved, e.g. problems with aggregation in aqueous solution, capacity loss, pressure drop in the column operation and economic and efficient and easy separation of NMOs from aqueous solutions. Such problems still remain an interesting and challenging task. Therefore fabrication of new NMOs-based composites of much better properties has been still in progress.

References

1. Hubbard AT (ed) (2002) Encyclopedia of surface and colloid science. Dekker, New York
2. Bergna HE (ed) (2005) Colloidal silica: fundamentals and applications. Taylor & Francis, Salisbury
3. Shpak AP, Gorbik PP (eds) (2010) Nanomaterials and supramolecular structures. Springer, Dordrecht
4. Blitz JP, Gun'ko VM (eds) (2006) Surface chemistry in biomedical and environmental science, NATO science series II: mathematics, physics and chemistry, vol 228. Springer, Dordrecht
5. Wiśniewska M, Nowicki P, Bogatyrov VM, Nosal-Wiercińska A, Pietrzak R (2016) Comparison of adsorption properties of Mg_xO_y–SiO_2 and Zn_xO_y–SiO_2 in the mixed oxide-poly(vinyl alcohol) system. Colloids Surf A Physicochem Eng Asp 492:12–18
6. Wiśniewska M, Bogatyrov V, Szewczuk-Karpisz K, Ostolska I, Terpiłowski K (2015) Adsorption mechanism of poly(vinyl alcohol) at the mixed oxide Cu_xO_y-SiO_2/aqueous solution interface. Appl Surf Sci 356:905–910
7. Klonos P, Pissis P, Gun'ko V, Kyritsisa A, Guzenko V, Pakhlov E, Zarko V, Janusz W, Skubiszewska-Zięba J, Leboda R (2010) Interaction of poly(ethylene glycol) with fumed silica and alumina/silica/titania. Colloids Surf A Physicochem Eng Asp 360(1–3):220–231
8. Voronin EF, Gun'ko VM, Guzenko NV, Pakhlov EM, Chuiko AA (2004) Interaction of poly (ethylene oxide) with fumed silica. J Colloid Interface Sci 279(2):326–340
9. Gun'ko VM, Zarko VI, Mironyuk IF, Goncharuk EV, Guzenko NV, Borysenko MV, Gorbik PP, Mishchuk OA, Janusz W, Leboda R, Skubiszewska-Zięba J, Grzegorczyk W, Matysek M, Chibowski S (2004) Surface electric and titration behaviour of fumed oxides. Colloids Surf A Physicochem Eng Asp 240(1–3):9–25

10. Wawrzkiewicz M, Wiśniewska M, Wołowicz A, Gun'ko VM, Zarko VI (2017) Mixed silica-alumina oxide as sorbent for dyes and metal ions removal from aqueous solutions and wastewaters. Micro Meso Mater 250:128–147
11. Wawrzkiewicz M, Wiśniewska M, Gun'ko VM, Zarko VI (2015) Adsorptive removal of acid, reactive and direct dyes from aqueous solutions and wastewaters using mixed silica-alumina oxide. Powder Technol 278:306–315
12. Gun'ko VM, Yurchenko GR, Turov VV, Goncharuk EV, Zarko VI, Zabuga AG, Matkovsky AK, Oranska OI, Leboda R, Skubiszewska-Zięba J, Janusz W, Phillips GJ, Mikhalovsky SV (2010) Adsorption of polar and nonpolar compounds onto complex nanooxides with silica, alumina, and titania. J Colloid Interface Sci 348(2):546–558
13. Di G, Zhu Z, Zhang H, Zhu J, Lu H, Zhang W, Qiu Y, Zhu L, Küppers S (2017) Simultaneous removal of several pharmaceuticals and arsenic on Zn-Fe mixed metal oxides: combination of photocatalysis and adsorption. Chem Eng J 328:141–151
14. Gao L, Li Q, Hu X, Wang X, Song H, Yan L, Xiao H (2016) One-pot synthesis of biomorphic Mg-Al mixed metal oxides with enhanced methyl orange adsorption properties. Appl Clay Sci 126:299–305
15. Lei C, Zhu X, Zhu B, Yu J, Ho W (2016) Hierarchical NiO–SiO_2 composite hollow microspheres with enhanced adsorption affinity towards Congo red in water. J Colloid Interface Sci 466:238–246
16. Skwarek E, Matysek–Nawrocka M, Janusz W, Zarko VI, Gun'ko VM (2008) Adsorption of heavy metal ions at the Al_2O_3-SiO_2/$NaClO_4$ electrolyte interface. Physicochem Probl Miner Process 42:153–164
17. Gun'ko VM, Nychiporuk YM, Zarko VI, Goncharuk EV, Mishchuk OA, Leboda R, Skubiszewska-Zieba J, Skwarek E, Janusz W, Yurchenko GR, Osovskii VD, Ptushinskii YG, Turov VV, Gorbik PP, Blitz JP, Gude K (2007) Relationships between surface compositions and properties of surfaces of mixed fumed oxides. Appl Surf Sci 253(6):3215–3230
18. Gun'ko VM, Zarko VI, Leboda R, Chibowski E (2001) Aqueous suspension of fumed oxides: particle size distribution and zeta potential. Adv Colloid Interface Sci 91:1–112
19. Gun'ko VM, Pakhlov EM, Skubiszewska-Zięba J, Blitz JP (2017) Infrared spectroscopy as a tool for textural and structural characterization of individual and complex fumed oxides. Vib Spectrosc 88:56–62
20. Gun'ko VM, Zarko VI, Leboda R, Marciniak M, Janusz W, Chibowski S (2000) Highly dispersed X/SiO_2 and C/X/SiO_2 (X=alumina, titania, alumina/titania) in the gas and liquid media. J Colloid Interface Sci 230(2):396–409
21. Sulym I, Sternik D, Oleksenko L, Lutsenko L, Borysenko M, Deryło-Marczewska A (2016) Highly dispersed silica-supported ceria–zirconia nanocomposites: preparation and characterization. Surf Interface 5:8–14
22. Gun'ko VM, Blitz JP, Bandaranayake B, Pakhlov EM, Zarko VI, Ya SI, Kulyk KS, Galaburda MV, Bogatyrev VM, Oranska OI, Borysenko MV, Leboda R, Skubiszewska-Zięba J, Janusz W (2012) Structural characteristics of mixed oxides MO_x/SiO_2 affecting photocatalytic decomposition of methylene blue. Appl Surf Sci 258:6288–6296
23. Reddy BM, Thrimurthulu G, Saikia P, Bharali P (2007) Silica supported ceria and ceria–zirconia nanocomposite oxides for selective dehydration of 4-methylpentan-2-ol. J Mol Catal A Chem 275:167–173
24. Reddy BM, Saikia P, Bharali P, Katta L, Thrimurthulu G (2009) Highly dispersed ceria and ceria–zirconia nanocomposites over silica surface for catalyticapplications. Catal Today 141:109–114
25. Navío JA, Colón G, Macías M, Sánchez-Soto PJ, Augugliaro V, Palmisano L (1996) ZrO_2–SiO_2 mixed oxides: surface aspects, photophysical properties andphotoreactivity for 4-nitrophenol oxidation in aqueous phase. J Mol Catal A Chem 109:239–248
26. Gao X, Fierro JLG, Wachs IE (1999) Structural characteristics and catalytic properties of highly dispersed ZrO_2/SiO_2 and $V_2O_5/ZrO_2/SiO_2$ catalysts. Langmuir 15:3169–3178

27. Basic characteristics of aerosil, Technical bulletin pigments, no. 11, Degussa AG, Hanau, 1997
28. https://www.wacker.com/cms/en/products/brands_2/hdk/hdk.jsp
29. https://www.aerosil.com/sites/lists/RE/DocumentsSI/Technical-Overview-AEROSIL-Fumed-Silica-EN.pdf
30. Pierson HO (1999) Handbook of chemical vapor deposition: principles, technology and applications. Noyes Publications, New York
31. Voronin EF, Pakhlo EM, Chuiko AA (1995) Chemisorption and hydrolysis of $TiCl_4$ on the surface of pyrogenic silica. Colloids Surf A Physicochem Eng Asp 101(2–3):123–127
32. Gun'ko VM, Zarko VI, Turov VV, Leboda R, Chibowski E, Holysz L, Pakhlov EM, Voronin EF, Dudnik VV, Gornikov YI (1998) CVD-titania on fumed silica substrate. J Colloid Interface Sci 198(1):141–156
33. Sulym I, Goncharuk O, Skwarek E, Sternik D, Borysenko MV, Derylo-Marczewska A, Janusz W, Gun'ko VM (2015) Silica-supported ceria–zirconia and titania–zirconia nanocomposites: structural characteristics and electrosurface properties. Colloids Surf A Physicochem Eng Asp 482:631–638
34. Sulym IY, Goncharuk O, Sternik D, Skwarek E, Derylo-Marczewska A, Janusz W, Gun'ko VM (2016) Silica-supported Titania–zirconia nanocomposites: structural and morphological characteristics in different media. Nanoscale Res Lett 11:111. https://doi.org/10.1186/s11671-016-1304-1
35. Sulim IY, Borysenko MV, Korduban OM, Gun'ko VM (2009) Influence of silica matrix morphology on characteristics of grafted nanozirconia. Appl Surf Sci 255:7818–7824
36. Bogatyrev VM, Gun'ko VM, Galaburda MV, Borysenko MV, Pokrovsky VA, Oranska OI, Polshin EV, Korduban OM, Leboda R, Skubiszewska-Zieba J (2009) Synthesis and characterization of Fe_2O_3/SiO_2 nanocomposites. J Colloid Interface Sci 338:376–388
37. Gun'ko VM, Bogatyrev VM, Borysenko MV, Galaburda MV, Sulim IY, Petrus LV, Korduban OM, Polshin EV, Zaulychnyy YV, Karpets MV, Foya OO, Myronyuk IF, Chelyadyn VL, UYa D, Leboda R, Skubiszewska-Zieba J, Blitz JP (2010) Morphological, structural and adsorption features of oxide composites with silica and titania matrices. Appl Surf Sci 256:5263–5269
38. Singh LP, Bhattacharyya SK, Ahalawat S, Kumar R, Mishra G, Sharma U, Singh G (2014) Sol-Gel processing of silica nanoparticles and their applications. Adv Colloid Interface Sci 214:17–37
39. Al Abdullah K, Awad S, Zaraket J, Salame C (2017) Synthesis of ZnO nanopowders by using sol-gel and studying their structural and electrical properties at different temperature. Energy Procedia 119:565–570
40. Imran M, Riaz S, Naseem S (2015) Synthesis and characterization of titania nanoparticles by sol-gel technique. Mater Today Proc 2(10):5455–5461
41. Harraz FA, Abdel-Salam OE, Mostafa AA, Mohamed RM, Hanafy M (2013) Rapid synthesis of titania–silica nanoparticles photocatalyst by a modified sol–gel method for cyanide degradation and heavy metals removal. J Alloys Compd 551:1–7
42. Tchounwou PB, Yedjou CG, Patlolla AK, Sutton DJ (2012) Heavy metals toxicity and the environment. EXS 101:133–164
43. Sharma K, Agrwal M (2005) Biological effects of heavy metals: an overview. J Environ BioI 26(2 suppl):301–313
44. Lakherwal D (2014) Adsorption of heavy metals: a review. Intern J Environ Res Develop 4 (1):41–48
45. Fu F, Wang Q (2011) Removal of heavy metal ions from wastewaters: a review. J Environ Manag 92(3):407–418
46. Agarwal SK (2009) Heavy metal pollution. APH Publishing Corporation, New Delhi
47. Lim AP, Aris AZ (2014) A review on economically adsorbents on heavy metals removal in water and wastewater. Rev Environ Sci Biotechnol 13:163–181

48. Da'na E (2017) Adsorption of heavy metals on functionalized-mesoporous silica: a review. Micro Meso Mater 247:145–157
49. Bakhiyi B, Gravel S, Ceballos D, Flynn MA, Zayed J (2018) Has the question of e-waste opened a Pandora's box? An overview of unpredictable issues and challenges. Environ Int 110:173–192
50. Hua M, Zhang S, Pan B, Zhang W, Lv L, Zhang Q (2012) Heavy metal removal from water/wastewater by nanosized metal oxides: a review. J Hazard Mater 211–212:317–331
51. Kurniawan TA, Chan GYS, Lo WH, Babel S (2006) Physico-chemical treatment techniques for wastewater laden with heavy metals. Chem Eng J 118:83–98
52. O'Connell DW, Birkinshaw V, O'Dwyer TF (2008) Heavy metal adsorbents prepared from the modification of cellulose: a review. Bioresour Technol 99:6709–6724
53. Aderhold D, Williams CJ, Edyvean RGJ (1996) The removal of heavy metal ions by seaweeds and their derivatives. Bioresour Technol 58(1):1–6
54. Fan M, Boonfueng T, Xu Y, Axe L, Tyson TA (2005) Modeling Pb sorption to microporous amorphous oxides as discrete particles and coatings. J Colloid Interface Sci 281:39–48
55. Hu J, Chen GH, Lo IMC (2005) Removal and recovery of Cr(VI) from wastewater by maghemite nanoparticles. Water Res 39:4528–4536
56. Martynyuk O, Kotolevich Y, Pestryakov A, Mota-Morales JD, Bogdanchikova N (2015) Nanostructures constituted by unusually small silica nanoparticles modified with metal oxides as support for ultra-small gold nanoparticles. Colloids Surf A Physicochem Eng Asp 487:9–16
57. Chen YH, Li FA (2010) Kinetic study on removal of copper (II) using goethite and hematite nano-photocatalysts. J Colloid Interface Sci 347:277–281
58. Hu J, Chen G, Lo IMC (2006) Selective removal of heavy metals from industrial wastewater using maghemite nanoparticle: performance and mechanisms. J Environ Eng-ASCE 132:709–715
59. Swallow KC, Hume DN, Morel FMM (1980) Sorption of copper and lead by hydrous ferric-oxide. Environ Sci Technol 14:1326–1331
60. Trivedi P, Dyer JA, Sparks DL (2003) Lead sorption onto ferrihydrite. 1. A macroscopic and spectroscopic assessment. Environ Sci Technol 37:908–914
61. Mishra SP, Vijaya (2007) Removal behavior of hydrous manganese oxide and hydrous stannic oxide for Cs (I) ions from aqueous solutions. Sep Purif Technol 54:10–17
62. Mishra SP, Dubey SS, Tiwari D (2004) Rapid and efficient removal of hg (II) by hydrous manganese and tin oxides. J Colloid Interface Sci 279:61–67
63. Takamatsu T, Kawashima M, Koyama M (1985) The role of Mn^{2+}-rich hydrous manganese oxide in the accumulation of arsenic in lake-sediments. Water Res 19:1029–1032
64. Tripathy SS, Bersillon JL, Gopal K (2006) Adsorption of Cd^{2+} on hydrous manganese dioxide from aqueous solutions. Desalination 194:11–21
65. Misono M, Ochiai EI, Saito Y, Yoneda Y (1967) A new dual parameter scale for strength of Lewis acids and bases with evaluation of their softness. J Inorg Nucl Chem 29:2685–2691
66. Dyer A, Pillinger M, Newton J, Harjula R, Moller T, Amin S (2000) Sorption behavior of radionuclides on crystalline synthetic tunnel manganese oxides. Chem Mater 12:3798–3804
67. Tsuji M, Komarneni S (1993) Selective exchange of divalent transition-metal ions in cryptomelane-type manganic acid with tunnel structure. J Mater Res 8:611–616
68. Ghaedi M, Niknam K, Shokrollahi A, Niknam E, Rajabi HR, Soylak M (2008) Flame atomic absorption spectrometric determination of trace amounts of heavy metal ions after solid phase extraction using modified sodium dodecyl sulfate coated on alumina. J Hazard Mater 155:121–127
69. Dadfarnia S, Shabani AMH, Shirie HD (2002) Determination of lead in different samples by atomic absorption spectrometry after preconcentration with dithizone immobilized on surfactant-coated alumina. Bull Kor Chem Soc 23:545–548

70. Shabani AMH, Dadfarnia S, Dehghani Z (2009) On-line solid phase extraction system using 1,10-phenanthroline immobilized on surfactant coated alumina for the flame atomic absorption spectrometric determination of copper and cadmium. Talanta 79:1066–1070
71. Afkhami A, Saber-Tehrani M, Bagheri H (2010) Simultaneous removal of heavy-metal ions in wastewater samples using nano-alumina modified with 2,4-dinitrophenylhydrazine. J Hazard Mater 181:836–844
72. Engates KE, Shipley HJ (2011) Adsorption of Pb, Cd, Cu, Zn, and Ni to titanium dioxide nanoparticles: effect of particle size, solid concentration, and exhaustion. Environ Sci Pollut Res 18:386–395
73. Liang P, Shi T, Li J (2004) Nanometer-size titanium dioxide separation/preconcentration and FAAS determination of trace Zn and Cd in water sample. Int J Environ Anal Chem 84:315–321
74. Mahdavi S, Jalali M, Afkhami A (2013) Heavy metals removal from aqueous solutions using TiO_2, MgO, and Al_2O_3 nanoparticles. Chem Eng Commun 200:448–470
75. Wang XB, Cai WP, Lin YX, Wang GZ, Liang CH (2010) Mass production of micro/nanostructured porous ZnO plates and their strong structurally enhanced and selective adsorption performance for environmental remediation. J Mater Chem 20:8582–8590
76. Ma XF, Wang YQ, Gao MJ, Xu HZ, Li GA (2010) A novel strategy to prepare ZnO/PbS heterostructured functional nanocomposite utilizing the surface adsorption property of ZnO nanosheets. Catal Today 158:459–463
77. Mahdavi S, Jalali M, Afkhami A (2012) Removal of heavy metals from aqueous solutions using Fe_3O_4, ZnO, and CuO nanoparticle. J Nanopart Res 14:846
78. Gao CL, Zhang WL, Li HB, Lang LM, Xu Z (2008) Controllable fabrication of mesoporous MgO with various morphologies and their absorption performance for toxic pollutants in water. Cryst Growth Des 8:3785–3790
79. Zhang F, Jin Q, Chan SW (2004) Ceria nanoparticles: size, size distribution, and shape. Jpn J Appl Phys 95:4319–4326
80. Bernal S, Calvino JJ, Cauqui MA, Gatica JM, Larese C, Omil JAP, Pintado JM (1999) Some recent results on metal/support interaction effects in NM/CeO_2 (NM: noble metal) catalysts. Catal Today 50:175–206
81. Contreras AR, Casals E, Puntes V, Komilis D, Sánches A, Font X (2015) Use of cerium oxide nanoparticles for the adsorption of dissolved cadmium(II), lead(II) and chromium(VI) at two different pHs in single and multi-component systems. Global NEST J 17:536–543
82. Eren E (2009) Removal of lead ions by Unye (Turkey) bentonite in iron and magnesium oxide-coated forms. J Hazard Mater 165:63–70
83. Eren E, Tabak A, Eren B (2010) Performance of magnesium oxide-coated bentonite in removal process of copper ions from aqueous solution. Desalination 257:163–169
84. Huang SH, Chen DH (2009) Rapid removal of heavy metal cations and anions from aqueous solutions by an amino-functionalized magnetic nano-adsorbent. J Hazard Mater 163:174–179
85. Oliveira LCA, Petkowicz DI, Smaniotto A, Pergher SBC (2004) Magnetic zeolites: a new adsorbent for removal of metallic contaminants from water. Water Res 38:3699–3704
86. Shin S, Jjang J (2007) Thiol containing polymer encapsulated magnetic nanoparticles as reusable and efficiently separable adsorbent for heavy metal ions. Chem Commun 41:4230–4232
87. Pereira L, Alves M (2015) Dyes – environmental impact and remediation. In: Malik A, Grohmann E (eds) Environmental protection strategies for sustainable development, strategies for sustainability. Springer, Dordrecht/Heidelberg/London/New York, pp 111–162
88. Gupta VK, Suhas (2009) Application of low-cost adsorbents for dye removal – a review. J Environ Manag 90(8):2313–2342

89. Elwakeel KZ (2009) Removal of Reactive Black 5 from aqueous solutions using magnetic chitosan resins. J Hazard Mater 167(1):383–392
90. Padmavathy S, Sandhya S, Swaminathan K, Subrahmanyam YV, Chakrabarti T, Kaul SN (2003) Aerobic decolorization of reactive azo dyes in presence of various cosubstrates. Chem Biochem Eng Q 17(2):147–151
91. Kumar Pandey A, Dubey V (2012) Biodegradation of azo dye reactive red BL by Alcaligenes sp. AA09. Int J Eng Sci 1(12):54–60
92. Dotto GL, Vieira MLG, Esquerdo VM, Pinto LAA (2013) Equilibrium and thermodynamics of azo dyes biosorption onto Spirulina platensis. Braz J Chem Eng 30(1):13–21
93. Saranraj P (2013) Bacterial biodegradation and decolourization of toxic textile azo dyes. Afr J Microbiol Res 7(30):3885–3890
94. Ciesielczyk F, Bartczak P, Zdarta J, Jesionowski T (2017) Active MgO-SiO_2 hybrid material for organic dye removal: a mechanism and interaction study of the adsorption of C.I. Acid blue 29 and C.I. Basic blue 9. J Environ Manag 204:123–135
95. Pal U, Sandoval A, Madrid SIU, Corro G, Sharma V, Mohanty P (2016) Mixed titanium, silicon, and aluminum oxide nanostructures as novel adsorbent for removal of rhodamine 6G and methylene blue as cationic dyes from aqueous solution. Chemosphere 163:142–152
96. Rasalingam S, Peng R, Koodali RT (2013) An investigation into the effect of porosities on the adsorption of rhodamine B using titania-silica mixed oxide xerogels. J Environ Manag 128:530–539
97. Tanzifi M, Yaraki MT, Kiadehi AD, Hosseini SH, Olazar M, Bharti AK, Agarwal S, Gupta VK, Kazemi A (2018) Adsorption of Amido black 10B from aqueous solution using polyaniline/SiO_2 nanocomposite: experimental investigation and artificial neural network modeling. J Colloid Interface Sci 510:246–261
98. Arshadia M, Vahid FS, Salvacion JWL, Soleymanzadeh M (2013) A practical organometallic decorated nano-size SiO_2-Al_2O_3 mixed-oxides for methyl orange removal from aqueous solution. Appl Surf Sci 280:726–736
99. Wawrzkiewicz M, Wiśniewska M, Gun'ko VM (2017) Application of silica–alumina oxides of different compositions for removal of C.I. Reactive black 5 dye from wastewaters. Ads Sci Technol 35(5–6):448–457
100. Abdelaal MY, Makki MSI, Sobahi TRA (2012) Modification and characterization of polyacrylic acid for metal ion recovery. Am J Polym Sci 2:73–78
101. Zheng H, Ma J, Ji F, Tang X, Chen W, Zhu J, Liao Y, Tan M (2013) Synthesis and application of anionic polyacrylamide in water treatment. Asian J Chem 25:7071–7074
102. Muppalaneni S, Omidian H (2013) Polyvinyl alcohol in medicine and pharmacy: a perspective. J Develop Drugs 2:3
103. Wiśniewska M, Bogatyrov V, Ostolska I, Szewczuk-Karpisz K, Terpiłowski K, Nosal-Wiercińska A (2016) Impact of poly(vinyl alcohol) adsorption on the surface characteristics of mixed oxide Mn_xO_y - SiO_2. Adsorption 22:417–423
104. Bogatyrov VM, Oranska IO, Gun'ko VM, Leboda R, Skubiszewska-Zięba J (2011) Influence of metal content on structural characteristics of inorganic nanocomposities M_xO_y/SiO_2 and $C/M_xO_y/SiO_2$. Chem Phys Tech Surf 2:135–146
105. Wiśniewska M, Ostolska I, Szewczuk-Karpisz K, Chibowski S, Terpiłowski K, Zarko VI, Gun'ko VM (2015) Investigation of the polyvinyl alcohol stabilization mechanism and adsorption properties on the surface of ternary mixed nanooxide AST (Al_2O_3-SiO_2-TiO_2). J Nanopart Res 17:12
106. Wiśniewska M, Szewczuk-Karpisz K, Ostolska I, Urban T, Terpiłowski K, Zarko VI, Gun'ko VM (2015) Effect of polyvinyl alcohol adsorption on the mixed alumina-silica-titania suspension stability. J Ind Eng Chem 23:265–272

107. Wiśniewska M, Chibowski S, Urban T (2015) Impact of polyacrylamide with different contents of carboxyl groups on the chromium(III) oxide adsorption properties in aqueous solution. J Hazard Mater 283:815–823
108. Wiśniewska M, Urban T, Grządka E, Zarko VI, Gun'ko VM (2014) Comparison of adsorption affinity of polyacrylic acid for surfaces of mixed silica-alumina. Colloid Polym Sci 292:699–705
109. Kasprzyk-Hordern B (2004) Chemistry of alumina, reactions in aqueous solution and its application in water treatment. Adv J Colloid Interface Sci 110:19–48